Preparation and Crystal Structure of Ruthenium Metaphosphate $Ru(PO_3)_3$ with an 8-fold Superstructure. Analysis of Structural Frustration with a Simple Model

Hideo Imoto,*,†,‡ Hiroshi Fukuoka,† Shigenori Tsunesawa,† Hisaya Horiuchi,‡ Takao Amemiya,‡ and Noboru Koga†,§

Department of Chemistry, School of Science, The University of Tokyo, Hongo, Tokyo 113, Japan, and Department of Chemistry, Faculty of Engineering Science, Osaka University, Toyonaka, Osaka 560, Japan

Received February 14, 1997[⊗]

Monoclinic $Ru(PO_3)_3$ was prepared as the third form of RuP_3O_9, and the structure was determined by the single-crystal X-ray technique. It contains infinite spiral chains of polyphosphate ions and RuO_6 octahedra as found in other C-form metaphosphates. While other C-form metaphosphates have 3-fold superstructures, monoclinic $Ru(PO_3)_3$ has a superstructure with an 8-fold *b*-axis. The space group is $P2_1/a$, and the cell parameters are $a = 10.578(5)$ Å, $b = 51.154(5)$ Å, $c = 9.394(4)$ Å, and $\beta = 97.74(4)°$. The comparison between the real structure and the parent subcell structure with the space group $I2/a$ shows that the deviations of the O1 atoms, which bridge two phosphorus atoms, are larger than those of other atoms. The displacements of the O1 atoms exhibit a static longitudinal sine wave along the *b*-axis with a wavelength of *b*/3. The bond angle P−O1−P is 180° in the parent subcell structure, and the shifts of the O1 atoms to attain more stable bond angles cause mechanical frustration, which leads to the superstructure. The observed superstructures of the monoclinic $Ru(PO_3)_3$ and C-form metaphosphates can be explained by a simple analytical model, in which neighboring O1 atoms are mechanically coupled through polyhedral chains to cause opposite displacements.

Introduction

Chemistry of transition-metal phosphates is now extensively being studied since the field has been found full of new compounds and interesting structures.[1] Recently we reported two ruthenium phosphates, cyclohexaphosphate $Ru_2(P_6O_{18})$ and triclinic metaphosphate $Ru(PO_3)_3$, which were the first reported ruthenium phosphates.[2] In this article, we describe another ruthenium phosphate, monoclinic metaphosphate $Ru(PO_3)_3$ (**1**). It is the stablest form among the three isomeric ruthenium phosphates at higher temperatures[2] and the first ruthenium phosphate that we have prepared. Powder X-ray studies indicated that its structure was similar to those of the C-form metaphosphates, $M(PO_3)_3$ (M = Al,[3] V,[4] Sc,[5] In,[6] Ti,[7] Mo,[8] Rh,[9] and Cr[10]). While these normal C-form metaphosphates have superstructures with a tripled *b*-axis, the powder pattern of **1** does not show clearly the reflection peaks expected for the tripled structure. The structural problem of the C-formlike $Ru(PO_3)_3$ had been unsettled until we could recently obtain single crystals suitable for X-ray studies. The analysis of the structure has revealed that the compound has an 8-fold *b*-axis.

Experimental Section

Preparation of 1. A mixture of ruthenium chloride hydrate (Aldrich) and phosphoric acid (85%) in the molar ratio of Ru:P = 1:5 was heated in a gold boat under a nitrogen stream at 430 °C for 5 days to give a red-black glassy material. Further heating of this material at 495 °C for 3 days followed by washing with ethanol for removal of unreacted phosphoric acid yielded a yellow powder of **1**. X-ray fluorescence analysis indicated that the product did not contain chlorine. The IR spectrum was similar to that reported for $Cr(PO_3)_3$.[11]

The compound could be prepared also by a reaction of soluble ruthenium oxide with phosphoric acid in a gold boat. However, the product was contaminated by a small amount of triclinic $Ru(PO_3)_3$.

Preparation of Single Crystals. Single crystals of **1** were obtained by using an amorphous precursor "$H_2RuP_3O_{10}$" prepared by the reaction of ruthenium chloride hydrate with phosphoric acid.[2] A mixture of the precursor and $NaNO_3$ (Ru:Na = 2:1) in a gold boat was heated under a nitrogen stream at 490 °C for 20 days. After a small amount of phosphoric acid was added, the mixture was heated at 450 °C for 4 days. The product was wrapped with a gold sheet, heated in an evacuated silica tube at 960 °C for 14 days, and washed with methanol−acetone to give orange single crystals of **1**. The crystals obtained by this method had very good quality for X-ray studies.

Single crystals of **1** could grow from the system without sodium if the conditions were suitable: The amorphous "$H_2RuP_3O_{10}$" described

† The University of Tokyo.
‡ Osaka University.
§ Present address: Faculty of Pharmaceutical Science, Kyushu University, Fukuoka 812-82, Japan.
⊗ Abstract published in *Advance ACS Abstracts,* August 1, 1997.

(1) Recent reviews: (a) Averbuch-Pouchot, M.-T.; Durif, A. *Topics in Phosphate Chemistry*; World Scientific: Singapore, 1996. (b) Durif, A. *Crystal Chemistry of Condensed Phosphates*; Plenum Press: New York, 1995. (c) Haushalter, R. C.; Meyer, L. M.; Zubieta, J. In *Early Transition Metal Clusters with π-Donor Ligands*; Chisholm, M. H., Ed.; VCH Publishers: New York, 1995; Chapter 5. (d) Rao, C. N. R.; Raveau, B. In *Transition Metal Oxides*; VCH Publishers: New York, 1995; Chapter 9.2.
(2) Fukuoka, H.; Imoto, H.; Saito, T. *J. Solid State Chem.* **1995**, *119*, 107.
(3) van der Meer, H. *Acta Crystallogr.* **1976**, *B32*, 2423.
(4) Middlemiss, N.; Hawthorne, F.; Calvo, C. *Can. J. Chem.* **1977**, *55*, 1673.
(5) Domanskii, A. I.; Shepelev, Yu. F.; Smolin, Yu. I.; Litvin, B. N. *Sov. Phys. Crystallogr. (Engl. Transl.)* **1982**, *27*, 140.
(6) Bentama, J.; Durand, J.; Cot, L. Z. *Anorg. Allg. Chem.* **1988**, *556*, 227. The coordinates reported in Table 2 of this article give abnormal distances for the atom In(2), and we have assumed the *y*-coordinate of the atom is 0.4098 instead of 0.1098 given in the table.
(7) Harrison, T. A.; Gier, T. E.; Stucky, G. D. *Acta Crystallogr., Sect. C* **1994**, *50*, 1643.
(8) Watson, I. M.; Borel, M. M.; Chardon, J.; Leclaire, A. *J. Solid State Chem.* **1994**, *111*, 253.
(9) Rittner, P; Glaum, R. *Z. Kristallogr.* **1994**, *209*, 162.
(10) Gruss, M.; Glaum, R. *Acta Crystallogr.* **1996**, *C52*, 2647.
(11) Rzaigui, M. *J. Solid State Chem.* **1990**, *89*, 340.

S0020-1669(97)00177-8 CCC: $14.00

above was heated in an evacuated silica tube at 980 °C for 17 days to yield orange single crystals of **1** on the wall of the silica tube. One of the single crystals obtained by this method was used for X-ray work described here. This method does not always give good single crystals. Heating the amorphous "$H_2RuP_3O_{10}$" in a silica tube yielded various compounds depending very delicately on the process of preparing the amorphous "$H_2RuP_3O_{10}$" and on the conditions of heating it.

When the product of a hydrothermal reaction of ruthenium chloride hydrate, $NaH_2PO_4 \cdot 2H_2O$, and phosphoric acid at 180 °C was heated at 1 100 °C in an evacuated silica tube, larger crystals of **1** were obtained. However, all of the crystals examined with an X-ray camera were rotation twins where the *c*-axis was the rotation axis.[12]

Structure Determination. Oscillation photographs around the *b*-axis and Precession photographs of the a^*-b^* plane of the crystal **1** showed satellite reflections, which we first interpreted as those due to the incommensurate superstructure along the *b*-axis. However, we found later that the observed superspots were consistent with 8-fold superstructure.

Single-crystal X-ray data were measured on a Rigaku AFC-5R diffractometer with Mo Kα radiation monochromated with graphite. Intensities of all reflections of the hemisphere ($\pm h,+k,\pm l$) in the 2θ range of $5° \le 2\theta \le 60°$ were collected in the ω-scan mode, a polyhedral crystal ($0.18 \times 0.26 \times 0.18$ mm) being used. Due to a very large length of the *b*-axis of the crystal, reflections *hkl* and $h,k \pm 1,l$ are very close in the reciprocal space, and the measured intensities of weaker reflections are inevitably influenced by neighboring stronger reflections. Therefore, we had to carefully select the reflections that could be used for the refinement. First, we omitted the reflections with asymmetric backgrounds. We judged a reflection was asymmetric if the following three conditions were all satisfied: (1) The higher background was larger than 3 times the lower background. (For each reflection, the background was measured before and after the scan of the peak, and we call the larger value the higher background and the other the lower background.) (2) The difference of the backgrounds was larger than 8 times the expected standard deviation (the square root of the sum of the variances of the backgrounds). (3) The higher background was larger than $^1/_{20}$ of the measured intensity of the peak. The number of the reflections omitted by this process was 73 among the 29 667 reflections. Then, the reflection data were corrected for absorption by the empirical φ-scan method[13] (relative transmission factor: 0.80−0.99) and equivalent reflections were averaged to yield 14 852 independent reflections ($R_{int}(F_o^2) = 0.034$). Among the reflections affected by the neighboring ones, the rejection of the asymmetric reflections removed only those whose neighboring affecting reflection was on the line along which the X-ray counter scanned by the ω-scan method. Therefore, we omitted the reflection *hkl* if the F_o of one of its neighboring reflections $h,k \pm 1,l$ was larger than 30.0 and also larger than 4 times the F_o of the reflection itself. The number of the reflections omitted in this second process was 2150 among 14 852 reflections. In the final refinements, 178 reflections that were not consistent with the systematic absences expected for the space group $P2_1/a$ were omitted, among which 52 reflections were observed. The number of the observed reflections with $|F_o| > 3\sigma(F_o)$ used for the refinements was 6973.

The observed systematic absence (*h*0*l*, *h* odd) showed that the structure had an *a*-glide plane. Furthermore, most of the reflections 0*k*0 (*k* odd) were not observed, which suggested the centrosymmetric space group $P2_1/a$. The existence of the screw axis could not be definitely deduced from the systematic absences due to the limited number of the reflections 0*k*0, and the structure was refined in both space groups. When the space group *Pa* was assumed, the refined structure gave a little better *R* values ($R = 0.049$, $R_w = 0.047$) for 12 297 observed reflections where Bijvoet pairs were not averaged. However, calculated P−O bond distances were scattered in abnormally wide ranges (1.41(2)−1.59(2) Å for P−O(−Ru) and 1.50(2)−1.68(2) Å for P−O(−P)). On the other hand, when the space group $P2_1/a$ was assumed, the *R* values were higher ($R = 0.058$, $R_w = 0.054$) for the same set of reflections, but all bond distances were reasonable. Consequently, we selected the space group $P2_1/a$.

Table 1. Crystallographic Data for **1** (Monoclinic $Ru(PO_3)_3$)

chem formula	O_9P_3Ru	fw	337.99
a	10.578(5) Å	space group	$P2_1/a$ (No. 14)
b	51.154(5) Å	*T*	297 K
c	9.394(4) Å	λ	0.7107 Å
β	97.74(4)°	ρ_{calcd}	3.57 g/cm^3
V	5037(3) Å^3	μ	32.8 cm^{-1}
Z	32	R, R_w	see Table 2

Table 2. *R*-Values for **1** (Monoclinic $Ru(PO_3)_3$)

type of reflcns	no. of reflcns	R^a	$R_w{}^b$
obsd all reflcns	6973	0.058	0.049
obsd sublattice reflcns[c]	1274	0.040	0.044
obsd superlattice reflcns[d]	5699	0.071	0.059
all reflcns[e]	10278	0.081	0.050
sublattice reflcns[c,e]	1621	0.045	0.044
superlattice reflcns[d,e]	8657	0.106	0.057

[a] $R = \sum(||F_o| - |F_c||)/\sum|F_o|$. [b] $R_w = [\sum w(|F_o| - |F_c|)^2/\sum w|F_o|^2]^{1/2}$, $w = 1/\sigma(F_o)^2$. [c] Reflections with indices *hkl*, $k = 8n$ (*n*: integer). [d] Reflections with indices *hkl*, $k \neq 8n$ (*n*: integer). [e] Reflections with $|F_o| < 3\sigma(F_o)$ were included, but those with negative measured intensities were omitted.

Initial positional parameters were obtained by transformation of the positional parameters of the subcell structure into those of the 8-fold cell. The parameters of the subcell structure were obtained by averaging the reported atomic parameters of $V(PO_3)_3$.[4] All atoms were isotropically refined by the full-matrix least-squares method with the ANYBLK program,[14] where scattering factors were taken from the standard source.[15] Empirical extinction correction was included in the refinements and the refined extinction parameter (*rT*) was $1.33(1) \times 10^{-6}$ cm^2.[16] The crystallographic data and final *R* values are shown in Tables 1 and 2, respectively.[17] The final positional and thermal parameters with interatomic distances and angles are given in the Supporting Information.

It should be noted that the intensities of the main reflections of **1** can be well reproduced by a very simple structure. The subcell structure of the present study ($b = 6.391$ Å) with a disorder of the position of the O1 atom can be refined with the main reflections to give good *R* values ($R = 0.055$ and $R_w = 0.066$ for 917 reflections). Better *R* values were obtained when we used reflection data obtained with a smaller crystal for which the effect of absorption was not strong ($R = 0.050$ and $R_w = 0.031$ for 796 reflections). If we had not noticed the existence of the superlattice reflections, we would have believed the average structure to be the true structure because it gave low *R* values.

Spectroscopic and Magnetic Measurements. The infrared absorption spectrum and the ultraviolet−visible spectrum of **1** were recorded on a Hitachi I-3000 spectrometer and a Hitachi U-3500 spectrometer, respectively. For the spectroscopic measurements, a finely powdered sample with KBr was pressed into a disk. Magnetic susceptibility was measured by the Faraday method on an Oxford Instruments magnetic susceptibility system with a 7-T superconducting magnet. The measured sample was fixed in a quartz cell with an aid of a small

(12) Giacovazzo, C. In *Fundamentals of Crystallography*; Giacovazzo, C., Ed.; Oxford University Press: Oxford, U.K., 1992; p 83.
(13) North, A. C. T.; Phillips, D. C.; Mathews, B. W. *Acta Crystallogr., Sect. A* **1968**, *24*, 351.
(14) H. Imoto, Program for the Least-squares Refinement of Atomic Parameters with Full Matrix and Block Diagonal Matrix Methods, University of Tokyo. Ver. 2.6, 1996.
(15) (a) *International Tables for Crystallography*; D. Kluwer: Dordrecht, The Netherlands, 1995; Vol. C, Tables 6.1.1.4. (b) *International Tables for X-Ray Crystallography*; Kynoch Press: Birmingham, England, 1974; Vol IV, Table 2.3.1.
(16) Zachariasen, W. H. *Acta Crystallogr.* **1967**, *23*, 558.
(17) If the reflections questionable concerning whether they are influenced by the neighboring reflections were included in the refinement, the converged *R* and R_w were 0.077 and 0.071, respectively, for 8517 observed reflections ($|F_o| > 3\sigma(|F_o|)$), where those with asymmetric backgrounds were omitted. The average deviation of the atomic sites obtained by this refinement from the corresponding site described in the Supporting Information was 1.3 pm, and the O2.6 atom showed the largest deviation (4.3 pm).

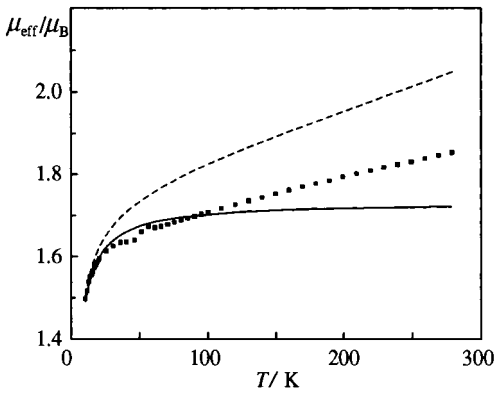

Figure 1. Effective magnetic moment μ_{eff} of **1**. Small squares show the observed values of μ_{eff} calculated by the equation $\{3kT(\chi-\chi_d)/N_A\}^{1/2}$. Here k is Boltzmann's constant, T is the temperature of the measurement, χ is the measured susceptibility, and N_A is Avogadro's number. The diamagnetic contribution χ_d was estimated by Pascal's law to be -1.13×10^{-4} emu/mol. The solid curve was calculated by the Curie law ($\mu_c/\mu_B = \{g^2s(s+1)T/(T-\Theta)\}^{1/2}$) with $s = {}^1/_2$, $g = 2$, and $\Theta = -3.55$ K. The broken curve was obtained by Kotani's theory ($\mu_K = \mu_c[\{1 + 8kT(1-p)/(3\lambda)\}/(1+2p)]^{1/2}$, $p = \exp\{-3\lambda/(2kT)\}$) with $\lambda = 1250$ cm^{-1}.

amount of Nujol. The background data for the cell and the Nujol were measured separately and subtracted from the raw data.

Results and Discussion

Preparation and Chemical Properties. Our first attempts to prepare ruthenium phosphate from ruthenium dioxide (rutile structure) were not successful. Ruthenium dioxide reacted very slightly with phosphoric acid or phosphorus(V) oxide and was reduced to metal when it was heated with ammonium phosphate. However, the reaction of ruthenium trichloride hydrate with phosphoric acid gave a yellow powder of **1**. The difficulty of the preparation of ruthenium phosphates from ruthenium dioxide indicates the high stability of the dioxide.

Compound **1** does not dissolve in mineral acids or strong alkaline solution. Reduction of the compound by a hydrogen flow (1 atm) at 1050 °C yielded a mixture of RuP_2 (marcasite structure)[18] and RuP (MnP structure).[19] Reduction of iron phosphate by hydrogen is one of the classical methods for preparing iron phosphides.[20]

Magnetic Properties and Visible Spectrum. The magnetic susceptibility of **1** approximately obeyed the Curie−Weiss law with a weak antiferromagnetic interaction ($\Theta = -3.55$ K) and indicated that each ruthenium atom (d^5) had one spin. At higher temperatures, the observed μ_{eff} values were larger than the spin-only values (1.73 μ_B) as shown in Figure 1 presumably due to the contribution of the orbital angular moment. The temperature dependence of the μ_{eff} value expected for a Ru^{3+} ion in the perfect octahedral environment calculated according to Kotani's method is illustrated in Figure 1.[21] At higher temperatures, the observed μ_{eff} values were lower than the values obtained by Kotani's method. The ruthenium atoms in **1** are not in perfect octahedra, and the orbital angular moment does not so completely contribute to the magnetic moments as assumed in Kotani's method.

The electronic spectrum of the compound had an absorption peak at 228 nm with a broad shoulder (370−470 nm) spread around 440 nm. This spectrum is very similar to that reported for the $Ru(H_2O)_6^{3+}$ ion in aqueous solution, which has an absorption peak at 225 nm and a weak absorption at 392 nm.[22] Following the analysis of the spectrum of the hexaaqua ion, we can assign the absorption of **1** with higher energy to a ligand-to-metal charge-transfer band and one with lower energy to a d−d band.

Table 3. Cell Constants and Space Groups of C-Form $M(PO_3)_3$

M	a/Å	b/Å	c/Å	β/deg	V/Å^3	SG[a]
Al[b]	10.423(3)	18.687(2)	9.222(1)	98.37(1)	1777	*Ia*
Rh[c]	10.481	19.065(9)	9.296(4)	98.03	1839(2)	*Ia*
Cr[d]	10.536	18.977(2)	9.347(1)	98.11	1850.2(3)	*Ia*
V[e]	10.615(2)	19.095(4)	9.432(1)	97.94(1)	1893	*Ia*
Ti[f]	10.730(2)	19.355(3)	9.551(2)	97.874(3)	1964.6	*Ia*
Mo[g]	10.819(1)	19.515(3)	9.609(1)	97.74(1)	2010(3)	*Ia*
In[h]	10.876(2)	19.581(2)	9.658(2)	97.77(1)	2038	*Ia*
Sc[i]	10.917	19.588	9.690	97.95	2052	*Ia*
Yb[j]	11.219(2)	19.983(3)	9.999(3)	97.30(2)	2223	$P2_1/c$
Ru[k]	10.578(5)	51.154(5)	9.394(4)	97.74(4)	5037(3)	$P2_1/a$
subcell	∼10.6	∼6.4	∼9.4	∼97.7	∼630	*I*2/*a*

[a] Space group. [b] Reference 3. The original space group was *Ic*. [c] Reference 9. The original space group was *Cc*. [d] Reference 10. The original space group was *Cc*. [e] Reference 4. The original space group was *Ic*. [f] Reference 7. The original space group was *Ic*. [g] Reference 8. [h] Reference 6. The original space group was *Ic*. [i] Reference 5. The original space group was *Cc*. [j] Reference 30. [k] This work.

Subcell Structure. While normal C-form metaphosphates have a 3-fold superstructure (space group *Ia*),[3−10] **1** has an 8-fold superstructure (space group $P2_1/a$). However, the structure of **1** is very similar to that of the normal C-form metaphosphates. The cell constants of these phosphates are compared in Table 3.

A unit cell of **1** contains eight subcells, the *b*-axes of which are $b/8$ (b_0) long. Because the atomic arrangements in the subcells of **1** are very similar to each other, the subcells can be regarded as distorted variations of a hypothetical subcell structure, which will be called the "parent structure". Furthermore, the subcells of **1** are very similar to those of the normal C-form metaphosphates. Therefore, it is reasonable to assume the parent structures of **1** and normal C-form metaphosphates to be isotypic. Then, the parent structures of these compounds must have all the symmetry elements found in both of them. To be the supergroup of the space groups $P2_1/a$ ($b = 8b_0$) and *Ia* ($b = 3b_0$), the space group of the parent structures is *I*2/*a*.

Though the parent structure has a small unit cell, we need the atomic coordinates of the structure in a big unit cell that has the same dimensions and the same symmetry ($P2_1/a$) as found for the real superstructure of **1**. The multiplicity of a general position of the small cell is eight while that of the big cell is four. Then, a general position in the small unit cell is converted into 16 independent positions in the big cell. They are expressed as (x_0, $(y_0 + n)/8$, z_0) and ($0.5 - x_0$, $(0.5 - y_0 + n)/8$, $0.5-z_0$), where x_0, y_0, and z_0 are the coordinates of the position in the small cell and n is an integer from 0 to 7. We label the atomic positions in the big cell by combining the name of the atomic positions in a small cell (Figure 2a) and the number of the sequence in generating the positions by the above expression. For example, the name O2.3 means that it is derived from the O2 atom in the small cell and generated by (x_0, $(y_0 + 3)/8$, z_0). If the atomic position is special, we obtained the sequence number after removing the duplicate positions from the list of the generated positions. In the parent structure, the atoms Ru and O1 are at an inversion center and the atom P1 is on a 2-fold rotation axis.

Since the atomic positions of the real superstructure have the one-to-one correspondence with those of the parent structure

(18) (a) Holseth, H.; Kjekshus, A. *Acta Chem. Scand.* **1968**, *22*, 3273. (b) Holseth, H.; Kjekshus, A. *Acta Chem. Scand.* **1968**, *22*, 3273.
(19) Rundqvist, S. *Acta Chem. Scand.* **1962**, *16*, 287.
(20) Struve, H. *Z. Prakt. Chem.* **1860**, *79*, 321.
(21) (a) Kotani, M. *J. Phys. Soc. Jpn.* **1949**, *4*, 293. (b) Kotani, M. *Prog. Theoret. Phys. Kyoto, Suppl.* **1960**, *14*, 293.
(22) Harzion, Z.; Navon, G. *Inorg. Chem.* **1980**, *19*, 2236.

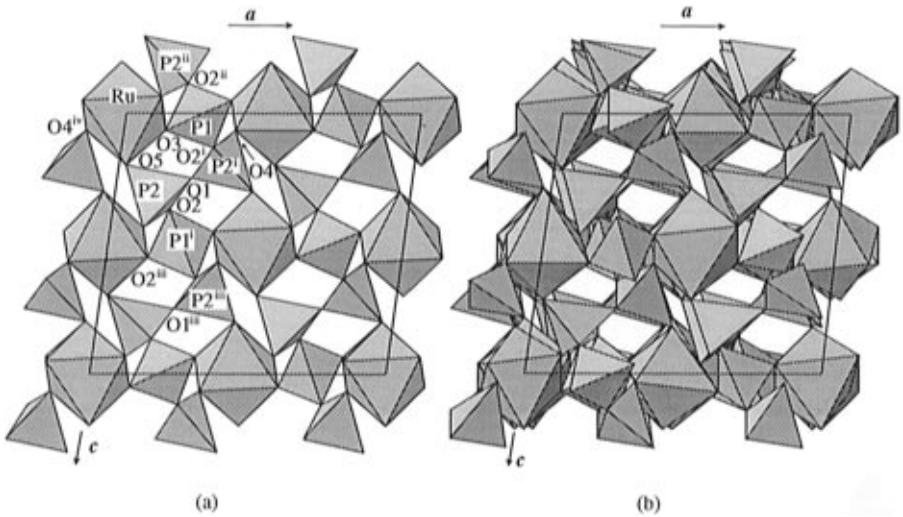

Figure 2. ORTEP drawing of **1** projected along the *b*-axis. (a) Parent structure calculated by averaging the subcells of monoclinic $Ru(PO_3)_3$ (**1**). Symmetry code: (i) $^1/_2-x$, $^1/_2-y$, $^1/_2-z$; (ii) x, $^1/_2-y$, $z-^1/_2$; (iii) $^1/_2-x$, y, $1-z$; (iv) $x-^1/_2$, $-y$, $z-^1/_2$. (b) Real structure of **1** illustrating the deviations of atomic sites from the parent structure.

Table 4. Atomic Coordinates of the Parent Structure of **1** (Monoclinic $Ru(PO_3)_3$)[a]

atom	*x*	*y*	*z*
Ru	0.0	0.0	0.0
P1	0.25	0.688 51	0.0
P2	0.138 97	0.160 89	0.313 37
O1	0.25	0.25	0.25
O2	0.192 36	−0.044 04	0.373 00
O3	0.147 07	−0.196 32	0.055 33
O4	0.382 31	0.211 27	0.064 43
O5	0.030 91	0.123 35	0.199 99

[a] Space group *I*2/*a*. Cell parameters: $a = 10.578$ Å, $b = 6.394$ Å, $c = 9.394$ Å, $\beta = 97.74°$. The atomic parameters were obtained by averaging those of the real structure.

described in the big cell, we use the same atomic labels for the real structure. This notation leads a natural classification of atomic positions in the real superstructure. For example, the atoms P2.0, P2.1, ..., and P2.15 make a group and they are called P2 atoms in the following discussion.

To obtain the coordinates of the parent structure in the small cell, we performed the reverse conversion of the atomic coordinates of the real structure and averaged them. The reverse conversion is (x, $8y - n$, z) for first eight atoms and ($0.5 - x$, $0.5 - 8y + n$, $0.5 - z$) for the rest. An atom at a special position can be reversely converted in two ways, and the averaging operation automatically leads to the fixed coordinates. The atomic coordinates of the parent structure of **1** calculated by this method are given in Table 4. We calculated the coordinates of the parent structures for normal C-form metaphosphates from the reported data by a similar method. The results show that all of the parent structures are very similar.

The parent structure of **1** is illustrated in Figure 2a, where the atomic labels used in this article are defined. Spiral metaphosphate chains containing a sequence −O2−P1−O2−P2−O1−P2− run along the *c*-axis. While O1 atoms and O2 atoms bridge two phosphorus atoms, other oxygen atoms are connected with a phosphorus atom and a ruthenium atom. Ruthenium atoms are octahedrally coordinated by oxygen atoms. The O1 atom is at an inversion center in the parent structure, and the crystallographic symmetry forces the bond angle P2−O1−P2 to be linear.

Superstructure. Since the number of bond distances and angles in **1** is too large, we group them and give minimum, maximum, and average values for each group in Table 5, where all bond distances or angles derived from the equivalent distances or angles in the subcell structure make a group. The standard deviation of bond distances in each group is small (0.007−0.016 Å), and most of the deviations of the bond angles of O−X−O (X = Ru and P) are smaller than those of oxygen

Table 5. Minimum, Maximum, and Average Bond Distances (Å) and Angles (deg) of Monoclinic $Ru(PO_3)_3$[a]

	n[b]	min[c]	max[c]	av	std[d]
Ru−O3	16	1.999(9)	2.057(9)	2.025	0.016
Ru−O4^{i}	16	2.000(8)	2.039(8)	2.020	0.011
Ru−O5	16	2.017(10)	2.078(9)	2.038	0.016
P1−O2	16	1.561(10)	1.603(10)	1.581	0.013
P1−O3	16	1.463(9)	1.504(9)	1.486	0.011
P2−O1	16	1.561(9)	1.609(8)	1.581	0.012
P2−O2	16	1.558(9)	1.604(10)	1.583	0.014
P2−O4	16	1.467(9)	1.500(9)	1.487	0.009
P2−O5	16	1.472(11)	1.498(10)	1.485	0.007
O3−Ru−O4^{i}	16	84.9(3)	93.6(3)	89.6	2.5
O3−Ru−O4^{iii}	16	87.1(3)	93.8(3)	90.4	1.9
O3−Ru−O5	16	83.4(3)	95.4(4)	89.6	3.8
O3−Ru−O5^{ii}	16	84.6(4)	96.6(3)	90.5	3.1
O4^{i}−Ru−O^{5}	16	85.8(3)	94.8(4)	90.6	2.8
O4^{i}−Ru−O5^{ii}	16	85.4(4)	93.0(4)	89.5	2.1
O3−Ru−O3^{ii}	8	174.5(4)	180.0	177.1	1.7
O4^{i}−Ru−O4^{iii}	8	173.2(4)	180.0	176.7	2.3
O5−Ru−O5^{ii}	8	172.6(3)	180.0	175.9	2.5
O2−P1−O2^{iii}	8	104.5(5)	108.4(5)	106.5	1.3
O2−P1−O3	16	101.2(5)	108.6(5)	105.4	2.1
O2−P1−O3^{iii}	16	106.3(5)	113.8(5)	109.6	2.4
O3−P1−O3^{iii}	8	116.9(5)	122.5(5)	119.6	1.8
O1−P2−O2	16	99.7(5)	104.3(5)	101.8	1.2
O1−P2−O4	16	106.5(5)	111.3(5)	109.3	1.2
O1−P2−O5	16	108.5(6)	112.7(5)	110.5	1.0
O2−P2−O4	16	105.8(5)	110.2(5)	108.0	1.4
O2−P2−O5	16	105.2(5)	114.9(5)	110.1	2.7
O4−P2−O5	16	114.4(5)	118.7(5)	116.3	1.1
P2−O1−P2	8	136.4(6)	151.6(7)	143.3	4.7
P1−O2−P2	16	134.8(6)	150.5(7)	143.1	4.8
Ru−O3−P1	16	131.6(6)	153.0(7)	141.4	6.3
Ru−O4−P2	16	128.1(6)	144.5(6)	136.8	5.6
Ru−O5−P2	16	133.1(5)	140.7(6)	136.4	2.1

[a] Bond distances or angles in the superstructure generated from the same or equivalent bond distances or angles in the subcell structure were grouped. Symmetry operation codes: (i) $x + ^1/_2$, $-y + ^1/_2$, z; (ii) $-x$, $-y$, $-z$; (iii) $-x + ^1/_2$, $y + ^1/_2$, $-z$. [b] The number of bond distances or angles in each group. [c] The standard deviations given in parentheses are obtained in the structure analysis, indicating the estimated errors. [d] The value is the standard deviation of the distribution of the bond distances or angles in each group.

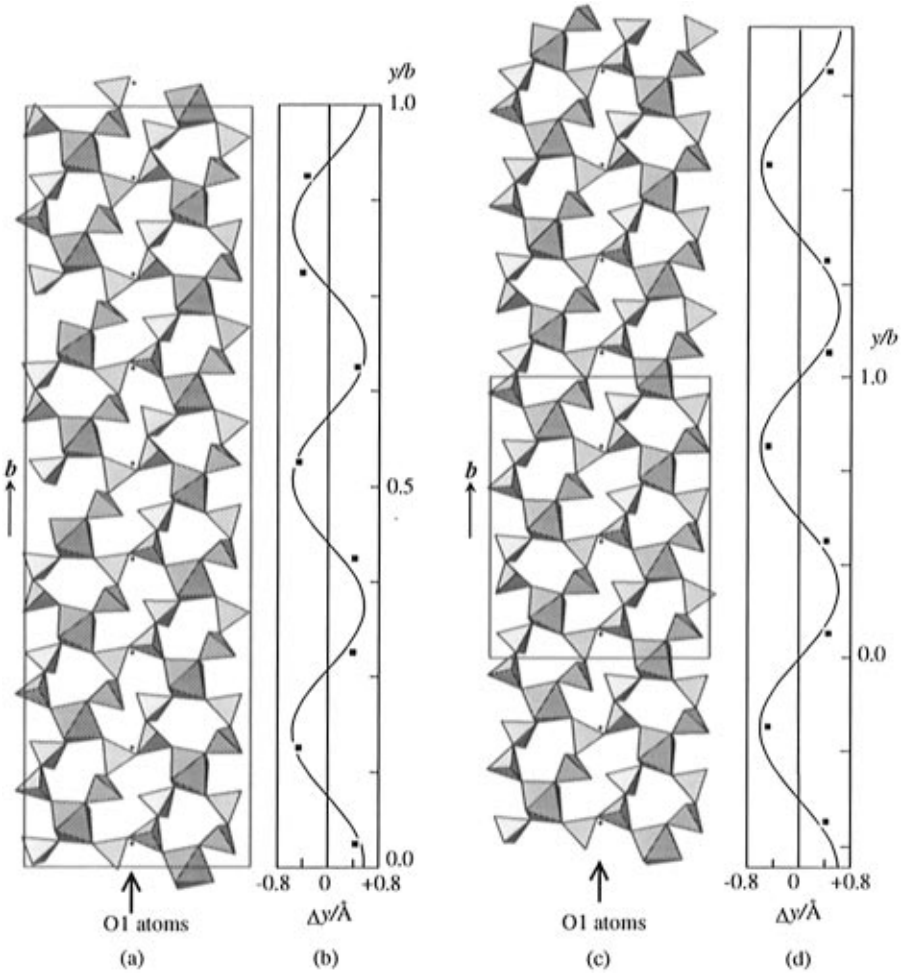

Figure 3. Comparison of the superstructures of **1** and $Rh(PO_3)_3$: (a) 101 section of the structure of **1**; (b) displacements of O1 atoms along the *b*-axis in **1** plotted against their *y*-coordinates; (c) 101 section of the structure of $Rh(PO_3)_3$; (d) displacements of O1 atoms along the *b*-axis in $Rh(PO_3)_3$ plotted against their *y*-coordinates. In (a) and (c), the small dots indicate the sites of the O1 atoms in the parent structure. In (b) and (d), the longitudinal displacement waves are illustrated as transversal waves.

Table 6. Average Displacements of Atomic Positions from the Parent Structure in $M(PO_3)_3$ (C-Form) (pm)[a]

	M	P1	P2	O1	O2	O3	O4	O5
Al[b]	13	18	10	48	33	23	31	25
Rh[c]	13	19	11	46	34	27	39	26
Cr[d]	13	18	10	46	36	26	34	26
V[e]	13	19	11	47	37	27	34	27
Ti[f]	15	21	10	52	38	27	34	27
Mo[g]	14	20	9	47	40	27	36	27
In[h]	16	22	9	54	41	33	35	28
Sc[i]	15	20	8	47	41	29	31	27
Ru[j]	13	19	12	57	35	27	38	25

[a] Labels of atoms are defined in Figure 2a. [b] Reference 3. [c] Reference 9. [d] Reference 10. [e] Reference 4. [f] Reference 7. [g] Reference 8. [h] Reference 6. [i] Reference 5. [j] This work.

atoms. The results indicate that the RuO_6 and PO_4 polyhedra are rigid. The averages of all bond distances in the superstructure are 2.028 Å for Ru−O, 1.486 Å for P−O(−Ru), and 1.582 Å for P−O(−P). These distances are similar to those observed in other ruthenium phosphates and ruthenium silicophosphate.[2,23]

We calculated the average displacement of each atom from the parent structures for **1** and for normal C-form metaphosphates (Table 6). In all of the phosphates in the table, the average displacement of the O1 atom is largest. The directions of the shifts of the O1 atoms are nearly along the *b*-axis. We will call a shift of an O1 atom toward the positive direction of the *b*-axis "up" and a shift in the reverse direction "down". Then, the sequence is up−down−up−up−down−up−down−down as shown in Figure 3a. On the other hand, the sequence in normal C-form metaphosphates (3-fold superstructure) is up−up−down−up−up−down (Figure 3c). In Figure 3, the amounts of the displacements of O1 atoms along the *b*-axis are plotted against their *y*-coordinates. The plots in Figure 3b,d indicate that the deviations of the O1 atoms make a static longitudinal sine wave along the *b*-axis. The wavelength is $^8/_3$ times of the length of the *b*-axis of the subcell (b_0) for **1** and 3 times for normal C-form metaphosphates.

The O1 atoms, which have the largest displacements, show a static wave with a wavelength of $^8/_3 b_0$. Then, it is plausible that other atoms have similar static displacement waves along the *b*-axis with the same wavelength. The existence of the wave in the whole structure can be directly proved by the intensity distribution of the superlattice reflections. The reflections with indices $k = 8k_0 \pm 3$ (k_0: integer) are much stronger than other superlattice reflections as shown in Table 7, which is expected from the theory for the superlattice reflections of the structure with a static wave along the *b*-axis with the wavelength of $^8/_3 b_0$.[24]

We discuss here the relations among the static displacement waves in the neighboring O1 columns running along the *b*-axis.

(23) Fukuoka, H.; Imoto, H.; Saito, T. *J. Solid State Chem.* **1996**, *121*, 247.

(24) Janssen, T.; Janner, A.; Looijengga-Vos, A.; de Wolff, P. M. In *International Tables for Crystallography*; Wilson, A. J. C., Ed.; Kluwer: Dordrecht, The Netherlands, 1995; Vol. C, p 799.

Table 7. Average Intensities of Satellite Reflections[a]

	j							
	0	1	2	3	4	5	6	7
no.	1987	1942	1912	1875	1845	1807	1767	1717
av int	1.000	0.013	0.034	0.225	0.005	0.187	0.019	0.016

[a] Average intensities of the reflections *hkl*, where $k = 8k_0 + j$ (k_0: integer). The values are normalized by the average of main reflections ($j = 0$). All reflections except for asymmetric ones are included.

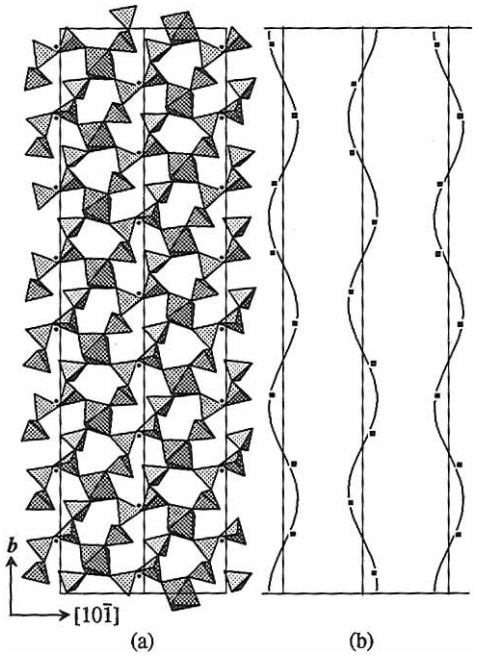

Figure 4. Arrangements of the displacement waves of **1** in a 101 layer: (a) 101 section of **1**, when the small dots indicate the positions of O1 atoms in the parent structure; (b) displacement waves of O1 atoms along the *b*-axis in **1** plotted against their *y*-coordinates, where longitudinal waves are illustrated as transversal waves.

As shown in Figure 4, the wave is approximately reverse in direction of the displacement to those in the neighboring columns in a 101 layer. In other words, the phases of the waves in the two neighboring columns are different by ca. π radians from each other. In normal C-form metaphosphates, the neighboring columns in a 101 plane are related by the body-centering translation, and the phases of their displacement waves have a difference of π radians exactly. Figure 5 illustrates the projection of the structure of **1** on a 100 plane showing the relation of the displacement waves in the adjacent 101 layers. It indicates that the phases of the waves in the neighboring 101 layers are different also by π radians. The difference is crystallographically fixed because the screw axis (2_1) running near the P1 atoms requires the neighboring displacement wave to be shifted by $b/2$ ($=4b_0$) along the *b*-axis. In normal C-form metaphosphates, similar phase differences are observed though the crystal symmetry does not force such phase differences. In conclusion, the phases of the displacement waves of the neighboring columns are always different by π radians in **1** and normal C-form metaphosphates.

Structural Frustration. In the parent structure of **1** and normal C-form metaphosphates, the O1 atoms are at an inversion center and have an unfavorable bond angle of 180°. In the real structures, they shift most greatly from the positions of the parent structure. Therefore, the origin of the deformation is presumed to be the O1 atoms and we start the description of the deformation of the C-form phosphates from the shift of an O1 atom.

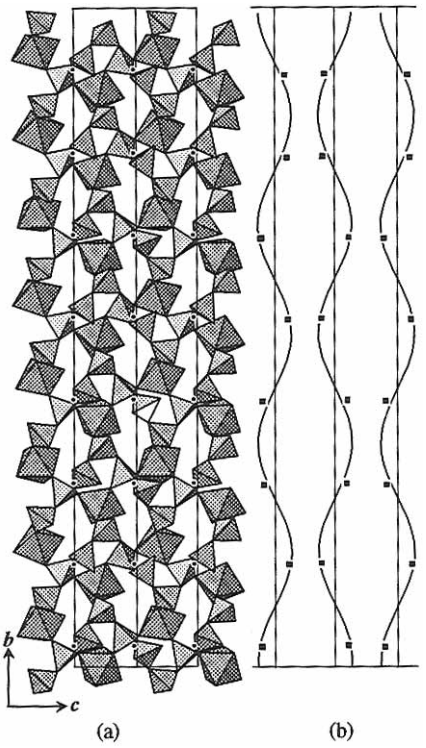

Figure 5. Arrangement of the displacement waves of **1** in the 100 plane: (a) 100 section of **1**, where the small dots indicate the positions of O1 atoms in the parent structure; (b) displacement waves of O1 atoms in the 100 plane, where longitudinal waves are illustrated as transversal waves.

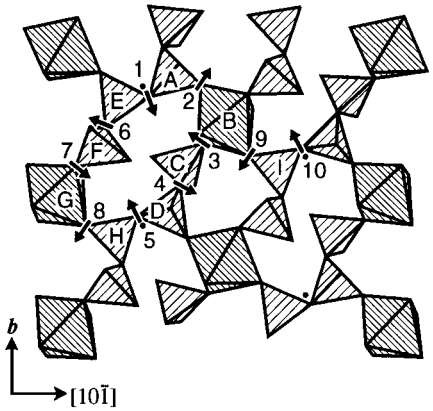

Figure 6. Mechanical transmission of the atomic movements caused by the displacement of an O1 atom in a single 101 layer. The mechanical transmissions through 1 → A → 2 → B → 3 → C → 4 → D → 5 and 1 → E → 6 → F → 7 → G → 8 → H → 5 lead to the vertical mechanical coupling between the O1 atoms while the transmission through 1 → A → 2 → B → 9 → I → 10 gives the diagonal coupling. Both couplings demand opposite displacements of the connected O1 atoms.

Since the bond angle of 180° is unfavorable for oxygen atoms, the O1 atom moves from an inversion center (1 in Figure 6). Then, the PO_4 tetrahedron (A in Figure 6) that contains the O1 atom has to rotate to keep the tetrahedral shape (2 in Figure 6). When the PO_4 tetrahedron A rotates, the MO_6 octahedron B that shares an oxygen atom with the tetrahedron has to rotate, too (3 in Figure 6). Thus, a shift of an O1 atom is transmitted mechanically to the neighboring polyhedra. We can see two routes that correlate the shifts of two O1 atoms neighboring in a column along the *b*-axis, 1→ A→ 2→ B→ 3→ C→ 4→ D→ 5 and 1→ E→ 6→ F→ 7→ G→ 8→ H→ 5 in Figure 6, and both of them lead to the reverse shifts of the neighboring O1 atoms. The mechanical transmission along the path 1→ A→

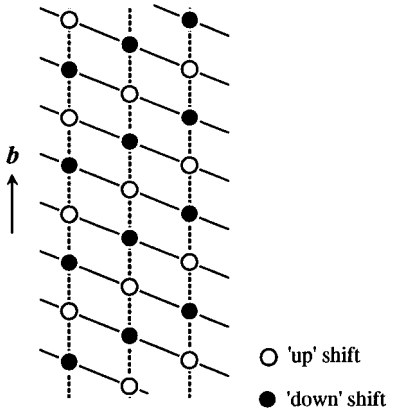

Figure 7. Hypothetical concerted shifts of the O1 atoms in a single 101 layer. Filled and open circles indicate "up" and "down" shifts of the O1 atom, respectively. Solid and broken lines represent diagonal and vertical couplings.

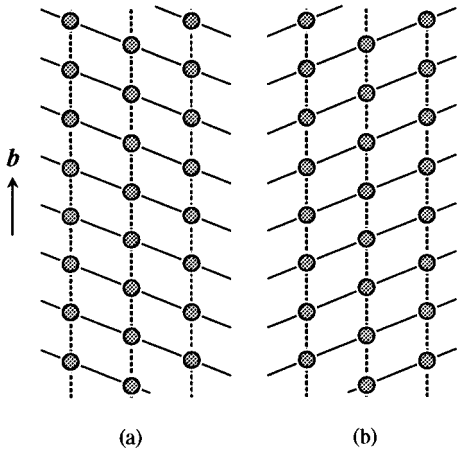

Figure 8. Schematic figure of a 101 layer of **1** and C-form metaphosphates showing the mechanical couplings between the O1 atoms. Circles indicate the sites of O1 atoms, and the connecting lines show the mechanical couplings between them. (solid line, diagonal coupling; broken line, vertical coupling): (a) A single 101 layer; (b) the 101 layer adjacent to the layer shown in (a). The two layers have opposite orientations.

2→ B→ 9→ I→ 10 correlates the movements of the O1 atoms in the neighboring column, and the O1 atoms prefer the shifts in opposite directions.

In summary, the O1 atoms in a 101 layer have two kinds of mechanical correlations. One is along the *b*-axis, and we will call it vertical coupling. Another is between the O1 atoms in the neighboring columns and will be called diagonal coupling. In both couplings, displacements in the opposite directions of the coupled O1 atoms are the stabler configuration. If only the atoms in a 101 layer are considered, the displacements of O1 atoms as shown in Figure 7 make all of the couplings satisfied. Therefore, if a single 101 layer were taken out of the real structures, the O1 atoms along the *b*-axis would shift in an up−down−up−down configuration and the structure would have a doubled *b*-axis. The real structures contradict this prediction, and we have to take interlayer interaction into account. As shown in Figure 8, the atomic arrangements of two adjacent 101 layers are not the same but related by a mirror perpendicular to the *b*-axis. These layers are connected by the mechanical coupling through 1→ A→ 11→ J→ 12→ K→ 13 as shown in Figure 9. The mechanical connection demands that the connected O1 atoms shift also in opposite directions and make the structure three-dimensionally coupled as schematically illustrated in Figure 10a.

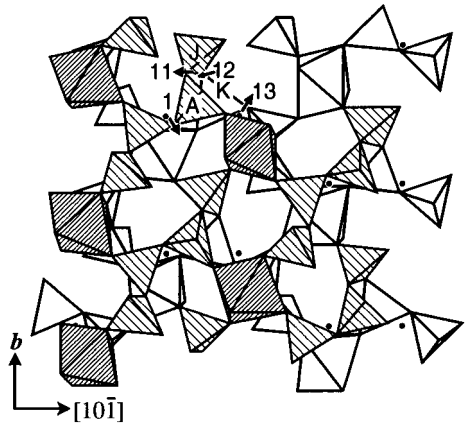

Figure 9. Mechanical transmission of the atomic displacements between the adjacent 101 layers. Two adjacent 101 layers are illustrated in the figure where the polyhedra in the front layer are hatched. Part of the front layer is omitted to show the back layer. The mechanical transmission through 1 → A → 11 → J → 12 → K → 13 leads to the interlayer mechanical coupling between the O1 atoms in the adjacent 101 layers.

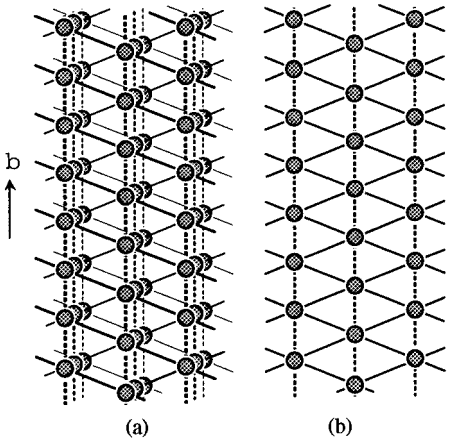

Figure 10. (a) Schematic figure of three adjacent 101 layers in **1** and C-form metaphosphates. Each layer is shown in Figure 7a,b. (b) Two-dimensional triangular system equivalent to the system of **1** and C-form metaphosphates if the negative couplings between the adjacent layers are completely fulfilled. Because vertical and diagonal couplings are both negative, the structure must have mechanical frustration.

Since the displacements of the O1 atoms adjacent along the *c*-axis are opposite in the real structures of **1** and normal C-form metaphosphates (Figure 5), we can regard the structure as made of chains of O1 atoms running along the *c*-axis, in which "up" and "down" displacements alternate. These chains are connected by diagonal and vertical couplings, and the problem becomes equivalent to that of a two-dimensional lattice as shown in Figure 10b. In other words, this system is made of the O1 atoms linked in a triangular way and each connection demands the opposite displacements of the connected O1 atoms. It is not possible to satisfy all of the requirements of the mechanical couplings, and the structure is mechanically frustrated. This situation is very similar to that observed in the spin system with *spin frustration*, where magnetic spins with negative coupling constants are arranged in a triangular lattice. Therefore, we propose to call the frustration of a whole structure caused by the mechanical interaction of the local atomic displacements *structural frustration*.

Recently, Khosrovani *et al.* determined the 3 × 3 × 3 superstructure of cubic zirconium pyrophosphate ZrP_2O_7 at room temperature and they ascribed the cause of the superstructure to the bending of the P−O−P angles which were 180° in the

parent structure.[25] The similarity of the C-form metaphosphate structure and the cubic ZrP_2O_7 is evident. In the parent subcell structures, both of the structures have linear P−O−P bonds, and in the real structure at room temperature, the bonds bend away to lead to the superstructures. In ZrP_2O_7, however, a ninth of the P−O−P angles are linear still in the superstructure, and at temperatures higher than 290 °C the superlattice reflections disappear, which indicates the long-range order of the displacements of the oxygen atoms is lost.

Mechanical Coupling Model. The structure has three kinds of mechanical couplings. The first is diagonal in a 101 layer, the second is vertical, and the third is interlayer. Due to these couplings, each couple of neighboring O1 atoms prefers shifting in opposite directions. If any one of the three couplings were negligibly weak, the structure would be free from mechanical frustration. An example is shown in Figure 7. The existence of the superstructure suggests that all of the couplings are not negligible.

Now we try to make a simple mathematical model of the frustrated three-dimensional structure illustrated in Figure 10a. The origin of the coordinate system is put on one of the O1 atoms. Then, the site of an O1 atom can be expressed by $j\boldsymbol{u} + k\boldsymbol{v} + l\boldsymbol{w}$ where $\boldsymbol{u}$, $\boldsymbol{v}$, and $\boldsymbol{w}$ are defined as $\boldsymbol{u} = (\boldsymbol{c} - \boldsymbol{a})/2$, $\boldsymbol{v} = \boldsymbol{b}_0$, and $\boldsymbol{w} = \boldsymbol{c}/2$, and we will denote the position by (j, k, l). The numbers j and l are integers, and the number k is an integer if j is even and a half-integer if j is odd. The vertical neighbors of an O1 atom at (j, k, l) are the atoms at $(j, k \pm 1, l)$ while the neighbors in the adjacent layers are at $(j, k, l \pm 1)$. The diagonally coupled neighbors are at $(j \pm 1, k \mp {}^1/_2, l)$ for even l and at $(j \pm 1, k \pm {}^1/_2, l)$ for odd l as illustrated in Figure 8. Since the strain due to the mechanical coupling is released by the opposite shifts of the O1 atoms connected by the coupling, the energy due to the mechanical frustration becomes smaller as the difference of the displacements of two neighboring O1 atoms increases from zero. It is not possible to estimate the function that describes how the distortion energy depends on the difference of the displacements of the neighboring O1 atoms. However, the function may be expanded in a power series containing only even powers and we assume, simply, that the first nonzero term, the square term, is important. We refer the energies to the energy of the crystal of the parent structure. Then, the average energy changes U, V, and W, which correspond to the couplings along $\boldsymbol{u}$ (diagonal), $\boldsymbol{v}$ (vertical), and $\boldsymbol{w}$ (interlayer), respectively, can be expressed by eqs 1−3. Here, N is the

$$U = -p\{\sum{}'(\Delta y_{(j+1)(k-1/2)l} - \Delta y_{jkl})^2 + \sum{}''(\Delta y_{(j+1)(k+1/2)l} - \Delta y_{jkl})^2\}/N,\ p > 0 \quad (1)$$

$$V = -q\sum(\Delta y_{j(k+1)l} - \Delta y_{jkl})^2/N,\ q > 0 \quad (2)$$

$$W = -r\sum(\Delta y_{jk(l+1)} - \Delta y_{jkl})^2/N,\ r > 0 \quad (3)$$

number of O1 atoms in the crystal. The summation $\sum$ runs all (j, k, l) sets for the O1 atom sites in the crystal while $\sum'$ and $\sum''$ run those with even and odd l values, respectively. The average energy change ΔE of the crystal due to the distortion is the sum of three terms, U, V, and W. Since it is difficult to treat this problem in a general form, we assume that the displacement Δy_{jkl} can be expressed as a single three-dimensional sine wave (eq 4) as found in the real structures. We can limit the parameter ν in the range of $0 \le \nu < 2\pi$ because substitution of $\alpha' = \alpha \pm \pi$ and $\nu' = \nu + 2\pi$ gives the same

$$\Delta y_{jkl} = a\sin(\alpha j + \nu k + \gamma l + \varphi) \quad (4)$$

$$a > 0 \quad -\pi < \alpha, \gamma, \varphi \le \pi$$

value of Δy_{jkl} for any set of (j, k, l). By eqs 1−4 we can get explicit expressions for U, V, and W. Because a crystal contains many O1 atoms, we can use the following relations:

$$\sum\sin(t_{jkl})\cos(t_{jkl})/N = \sum{}'\sin(t_{jkl})\cos(t_{jkl})/N = \sum{}''\sin(t_{jkl})\cos(t_{jkl})/N = 0 \quad (5)$$

$$\sum\cos^2(t_{jkl})/N = \sum\sin^2(t_{jkl})/N = {}^1/_2 \quad (6)$$

$$\sum{}'\cos^2(t_{jkl})/N = \sum{}'\sin^2(t_{jkl})/N = \sum{}''\cos^2(t_{jkl})/N = \sum{}''\sin^2(t_{jkl})/N = {}^1/_4 \quad (7)$$

$$\text{where } t_{jkl} = \alpha j + \nu k + \gamma l + \varphi$$

Then, the expressions of U, V, and W can be reduced into the following simple forms, where the calculations are tedious and we used a computer algebra program:[26]

$$U = -pa^2\{1 - \cos\alpha\cos(\nu/2)\} \quad (8)$$

$$V = -qa^2(1 - \cos\nu) \quad (9)$$

$$W = -ra^2(1 - \cos\gamma) \quad (10)$$

Because the parameter γ appears only in the expression for W, minimization of W determines the value of γ to be equal to π. This is what we observe in the real structures as illustrated in Figure 5.

The parameter α influences only U, and $\cos(\nu/2)$ is positive because ν is in the range of $0 \le \nu < 2\pi$. Then, U gets the minimum when $\alpha = \pi$. This is also what we observe in the real structures as shown in Figure 4. Replacement of the parameter α and γ with π gives the expression of ΔE as eq 11.

$$\Delta E = -qa^2\{\theta + 1 + \theta\cos(\nu/2) - \cos\nu\} - 2ra^2 \quad (11)$$

$$\theta = p/q$$

The condition for the minimum of ΔE leads to eq 12. Therefore,

$$\nu = 2\arccos(\theta/4) \quad (12)$$

the wavelength λ of the displacement wave is given by eq 13.

$$\lambda/b_0 = \pi/\arccos(\theta/4) \quad (13)$$

Figure 11 illustrates the relation between θ and λ. According to eq 13, if the diagonal coupling is stronger than the four times of the vertical coupling ($\theta \ge 4.0$), the wavelength becomes infinite, and only "up" or "down" shifts occur in a column along the b-axis. Because diagonally neighboring O1 atoms are connected through a shorter path than the vertically connected neighbors, it is very reasonable that the coupling p is greater than the coupling q (i.e. $\theta > 1.0$). If the strength of the diagonal coupling is twice that of the vertical coupling ($\theta = 2$), the wavelength λ/b_0 becomes 3, as we observe in normal C-form metaphosphates. The observed wavelength in **1** ($\lambda/b_0 = {}^8/_3$) is attained if the parameter θ has a smaller value ($\theta = 1.53$).

(25) Khosrovani, N.; Korthuis, V.; Sleight, A. W.; Vogt, T. *Inorg. Chem.* **1996**, *35*, 485.

(26) *Maple V Release 4*: *Computer Algebra system*; Waterloo Maple Inc: Waterloo, Canada, 1996.

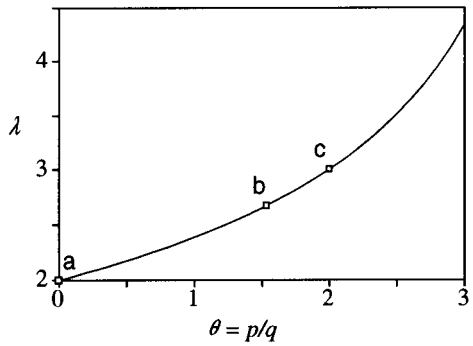

Figure 11. Relation between the parameter θ and the wavelength (λ) of the modulation expected from the simple model. The parameter θ is the ratio of the diagonal coupling constant to the vertical coupling constant. The point (a) represents a structure in which the "up" shift and the "down" shift alternate as shown in Figure 12a. The points (b) and (c) correspond to the superstructures of **1** ($\lambda = {}^{8}/_{3}$) and C-form metaphosphates ($\lambda = 3$), respectively, which are illustrated in Figure 12b,c.

Our discussion is based on a very simple model, and we do not think that the results derived from the model are quantitatively exact. However, the model predicts two important features of the superstructures in **1** and normal C-type metaphosphates: (1) The wavelength of the displacement waves along the *b*-axis can vary depending on the ratio of the strengths of the mechanical couplings. (2) The waves in the neighboring columns have always opposite phases. These predictions are consistent with the real superstructures of these metaphosphates.

Two-Site Model. In the model discussed above, we have exaggerated the continuous nature of the displacements of the O1 atoms to make the model easily processed analytically. We can take another approach to the problem, where we assume only two positions ("up" and "down") are possible for each O1 atom and count the numbers of satisfied and unsatisfied couplings. In this approach, we cannot predict the configurations of the superstructures, but we can explain the changes of the superstructure as the parameter θ increases. Figure 12 summarizes the configurations of the displacements of the O1 atoms. If the vertical coupling is much stronger than the diagonal coupling, "up" displacements and "down" displacements alternate along the *b*-axis, which means the wavelength is $2b_0$. As the diagonal coupling becomes stronger, the wavelength gets longer. The arrangements in **1** and normal metaphosphates are illustrated in Figure 12b,c, respectively. Finally, if the strength of the diagonal coupling is much larger, all O1 atoms in a column along the *b*-axis shift in the same direction (Figure 12d). The ratios of the couplings connecting oppositely displaced O1 atoms (satisfied couplings) to all couplings are also given in the figure. As we expect, the ratio of the satisfied diagonal couplings increases as the θ parameter while the ratio for the vertical coupling shows a reverse tendency.

The mechanical system described in the two-step model is similar to the Ising model of spin systems. If we reduce the system into the two-dimensional lattice as shown in Figure 10b, it is comparable to the triangular spin lattice, where magnetic spins have antiferromagnetic couplings with neighboring spins. In the triangular spin system, all couplings between nearest neighbors have the same strength, which corresponds to $\theta = 2$ in the present system because the number of the vertical couplings is twice the number of the diagonal couplings of each type. In the exact triangular Ising system, the spins are not ordered.[27] However, if a small positive next-neighbor coupling is introduced, ferrimagnetic ordering becomes stable, and the resulting arrangement of the spins is similar to the pattern shown in Figure 12c.[28]

$Ru(PO_3)_3$ vs Normal C-Form Phosphates. All single crystals of **1** have shown an 8-fold superstructure, while all C-form metaphosphates with superstructure have tripled b-axes. However, the local geometries of the two superstructures are almost identical. All average bond angles of **1** except for *trans*-O−M−O angles are between the corresponding angles of $Mo(PO_3)_3$ and $Rh(PO_3)_3$ (Table 8), and average geometries do not indicate any special feature in the structure of **1** compared to the normal C-form metaphosphates. Subtle conditions seem to determine whether the 3-fold or 8-fold superstructure is adopted by a particular metaphosphate. Discussion in the previous sections indicates that stronger vertical couplings compared to the diagonal couplings induce the 8-fold superstructure instead of the 3-fold one. Then, the problem is how the strengths of the vertical and diagonal couplings are determined. The diagonal coupling is transmitted through a *trans*-O−M−O linkage of a metal octahedron, and its strength is determined by the rigidity of the *trans*-O−M−O angle (Figure 13). This prediction is supported by comparing the geometries of the MO_6 octahedra on the routes of the mechanical transmission of the satisfied couplings and those on the routes of unsatisfied couplings. In **1**, the *trans*-O4−Ru−O4 angles in the unsatisfied couplings are significantly bent (173.2(4), 173.5(3), and 174.9(4)°) while the corresponding angles in the satisfied couplings are between 177.4 and 180° (average 178.4°). Therefore, the O4−Ru−O4 angles have some strain in the unsatisfied couplings, and the strength of the diagonal coupling is mainly determined by the energy to bend the *trans*-O−Ru−O angle. On the other hand, the vertical coupling is caused by mechanical connection through a tetrahedron of the P1 atom and a *cis*-O−Ru−O linkage (Figure 13). The phosphorus atoms that are on the paths of the unsatisfied couplings are P1.2 and P1.7. Their coordination tetrahedra have a small O−P1−O angle (102.1(5) and 101.2(5)°) while the minimum O−P1−O angles in other $P1O_4$ tetrahedra are larger than 103.2° (average 104.4°). These bond angles indicate that the $P1O_4$ tetrahedra in the unsatisfied vertical couplings have some strain. In contrast, the octahedra in the unsatisfied couplings are not much deformed. The angles of *cis*-O3−Ru−O4 are within 90.0 ± 3.5°, and the octahedra are not effective in releasing the strain in the unsatisfied vertical coupling. Therefore, the geometries indicate that the strength of the vertical coupling is mainly determined by the rigidity of the O−P1−O angle. In conclusion, the 8-fold superstructure is stabilized compared to the 3-fold one by two factors: (a) soft *trans*-O−M−O angles; (b) rigid O−P1−O angles. The reason that only ruthenium metaphosphate satisfies these conditions has not been well solved as yet.

Symmetry of the C-Form Metaphosphate Structures. As discussed above, all of the C-form phosphates have very similar parent structures of the *I*2/*a* symmetry, where the P1 atoms are on the 2-fold rotation axis. In the real structure, however, the shifts of the O1 atoms rotate the tetrahedra of the P1 atom around the normal of the 101 plane, and the 2-fold rotation symmetry is destroyed. Possible subgroups of the space group *I*2/*a* with $\boldsymbol{a} = \boldsymbol{a}_0$, $\boldsymbol{b} = n\boldsymbol{b}_0$, and $\boldsymbol{c} = \boldsymbol{c}_0$, ($\boldsymbol{a}$, $\boldsymbol{b}$, $\boldsymbol{c}$, unit cell vectors of the superstructure; $\boldsymbol{a}_0$, $\boldsymbol{b}_0$, $\boldsymbol{c}_0$, unit cell vectors of the subcell) depend on whether the number *n* is even or odd. If *n* is odd, the space group of the superstructure is *I*2/*a* or any of its t subgroups.[29] If we exclude the space groups that have the 2-fold

(27) (a) Wannier, G. H. *Phys. Rev.* 1950, *79*, 357. (b) Wannier, G. H. *Phys. Rev. B* **1973**, *7*, 5017.
(28) Mekata, M. *J. Phys. Soc. Jpn.* **1977**, *42*, 76.

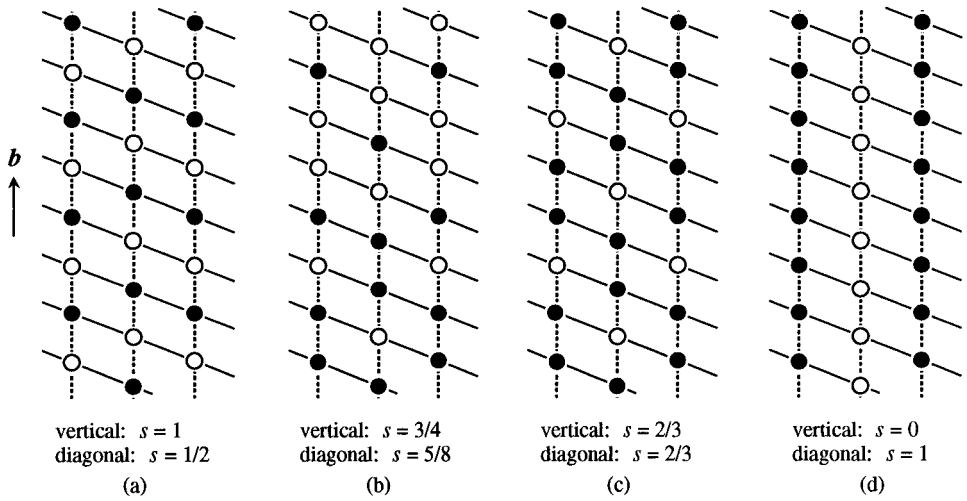

Figure 12. Configurations of the shifts of O1 atoms in a 101 layer. Filled and open circles indicate "up" and "down" shifts of the O1 atom, respectively. Solid and broken lines represent diagonal and vertical couplings. The parameter *s* is defined as (number of satisfied coupling)/(number of all couplings). (a) Configuration expected for strong vertical coupling ($\lambda = 1$). (b) Configuration in **1** ($\lambda = {}^{8}/_{3}$). (c) Configuration in normal C-form metaphosphates ($\lambda = 3$). (d) Configuration expected for strong diagonal coupling.

Table 8. Average Bond Angles in $M(PO_3)_3$ with Standard Deviations in Parentheses (deg)

	$Mo(PO_3)_3$	$Ru(PO_3)_3$	$Rh(PO_3)_3$
M(cis)	90.04(3.10)	90.03(2.84)	90.02(2.63)
M(trans)	175.06(2.06)	176.58(2.29)	176.34(1.96)
P1	109.34(4.89)	109.35(5.33)	109.35(5.64)
P2	109.28(4.64)	109.30(4.52)	109.31(4.42)
O1	141.03(3.09)	143.25(4.72)	143.04(4.01)
O2	142.05(5.50)	143.13(4.83)	143.97(4.67)
O3	147.69(6.60)	141.39(6.32)	139.49(6.68)
O4	140.11(5.58)	136.81(5.62)	135.57(5.00)
O5	141.29(2.28)	136.44(2.10)	134.84(1.87)

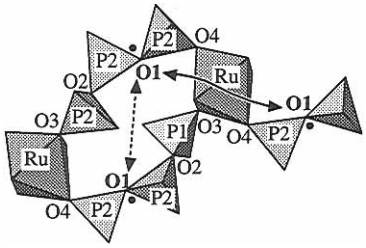

Figure 13. Part of the 101 layer of **1** illustrating the transmission paths of a vertical coupling (broken line) and a diagonal coupling (continuous curve) between the neighboring O1 atoms.

rotation axis, the possible space groups with the highest symmetry are *Ia*, $P2_1/c$, and $P2_1/a$. The last is not suitable because it requires some of the O1 atom at the inversion center. The space group *Ia* is observed for most of the C-form metaphosphates. The space group $P2_1/c$ was reported for $Yb(PO_3)_3$[30] though the assignment of the space group had some ambiguity.[31] On the other hand, if the number *n* is even, the possible space groups are $P2_1/a$, $P2_1/c$, or any of the t subgroups of them. However, the space group $P2_1/c$ requires some of the O1 atoms at the inversion center and the allowed space group with the highest symmetry is only $P2_1/a$, which is the one found for **1**. In conclusion, the possible space groups for C-form metaphosphates with the highest symmetries are *Ia* with odd *n*, $P2_1/c$ with odd *n*, and $P2_1/a$ with even *n*, and all of them have been reported for real structures.

Conclusion

Many stoichiometric oxides including silicates and phosphates are reported to have superstructures. In most of these compounds, the causes of the superstructures are not attributable to the electronic structures and must be some local mechanical frustration. However, the mechanism how the mechanical frustration leads to the superstructure has not been well understood due to the complexity of the real structures.

The superstructures of **1** and that of the C-form metaphosphates are different only in the wavelength of modulation. They are simple superstructures in some aspects: (1) Only O1 atoms connecting two phosphorus atoms are mechanically frustrated. They have bond angles of 180° in the parent structure. (2) The displacements of the O1 atoms are mainly along the *b*-axis. (3) The superstructures have only one main modulation wave.

Owing to these simple characters, we can construct a mathematical model, which reveals fundamental features of these superstructures. The origin of these superstructures is the linear bond angles of oxygen atoms. Because the displacements of the oxygen atoms induce the consecutive rotations of connected MO_6 and PO_4 polyhedra, the oxygen atoms are mechanically coupled. If the couplings are not consistently satisfied by any set of displacements of the frustrated atoms in a unit cell, a superstructure appears. We can say, in short, "structural frustration causes the superstructure". Many superstructures of oxides seem to have the same mechanism. The most important examples are perovskite-type compounds and three forms of silica. All these compounds have linear bond angles of oxygen atoms in high-temperature structures, which can be regarded as the parent structure, and have many kinds of superstructures at lower temperatures.

Acknowledgment. We thank Prof. Taro Saito for helpful discussions and Prof. Hiroki Oshio for discussion and information about spin frustration.

Supporting Information Available: An X-ray crystallographic file, in CIF format, is available. Access ordering information is given on any current masthead page.

IC9701773

(29) *International Tables for Crystallography*; Hahn, T., Ed.; Reidel: Dordrecht, Holland, 1983; Vol A, pp 167, 183.
(30) Hong, H. Y.-P. *Acta Crystallogr., Sect. B* **1980**, *30*, 1857.
(31) Bagieu, M. Ph.D. Thesis, University of Grenoble, Grenoble, France, 1980.